

# Compact Electromagnetic XY Stage with Nano Scale Resolution and Vibration Resistance

Kyoung Il Lee\*, Seong Hyun Kim\*, Jin Woo Cho\*, Jin Koog Shin\*, Jong-Chul Yoo\*\*, and Young Jin Choi\*\*

\*Korea Electronics Technology Institute, Korea, leeki@keti.re.kr

\*\*Myongji University, Korea, jini38@mju.ac.kr

## ABSTRACT

The design, fabrication, and the measurement results of an electromagnetic XY stage are presented. The device has an anti vibration structure and shows a high fill factor of 45% due to its unique structure. The device consists of a top substrate on a flexure holding magnets, a spacer, and a PCB including multilayered coils. The top substrate is forced to move in the opposite direction of the magnets by applying a current in the coil. The flexure is designed to have no net torque around its pivot under an external acceleration showing a good vibration resistance. The modal analysis shows that the high order resonance can be placed above 3 kHz by gimbal. The FEM analysis shows that the vibration under 1G acceleration can be suppressed below 10 nm. The stage shows a good linearity and a low average power consumption of 60 mW for 0.068 mm x 0.068 mm scanning, which is acceptable for a portable application. The first resonance frequency is 186 Hz, which is lower than expected due to the spring width decrease.

**Keywords:** electromagnetic actuator, SPM, data storage

## 1 INTRODUCTION

The evolution of flash memory technology seems to be no bound but the extremely high cost for EUV line makes the commercialization of it very risky. So the new solution for portable data storage with very large capacity is required to meet the improvement of next-generation multimedia mobile platforms. A Probe-based data storage is known to be one of the candidates because very small bits for high data density can be recorded and read by extremely sharp tips.[1-3] But the mechanical reliability becomes very important since it requires two dimensional scanning motion.

A probe-based data storage usually consists of an array of reading/writing probes, a storage medium, circuits for control, and an actuator. The actuator is used to make a relative motion between the medium and the array of probes. XY translation is preferred because 2D array of the probes is indispensable for the probe-based storage to achieve a high data transfer rate. So, one of the barriers to realizing a probe storage is to fabricate a reliable high performance media XY stage with low power consumption. The requirements of the actuator for the probe-based

storage are a large stroke covering the pitch of probes, a high resonant frequency for short access time, a high positioning resolution for good signal-to-noise (S/N) ratio, robustness against external vibration and shock, and a small form factor.

Various actuators have been proposed to meet these requirements with electrostatic [4, 5], piezoelectric [6], and electromagnetic [7-9] mechanism. Electromagnetic actuators can be driven with a low voltage and shows a very good linearity useful for servo control. Pantazi et al. have developed an electromagnetic actuator with low power consumption and high vibration resistance but it has shown a low fill factor limiting the area for data recording. Also it needs a bonding process with lateral alignment and it makes the device thick[9].

In this paper, we present the design, fabrication and measurement results of a miniature electromagnetic XY stage with high fill factor and vibration resistance for probe-based data storage.

## 2 DESIGN

A schematic view of the stage is illustrated in Figure 1. The device consists of a top substrate, a silicon flexure holding 2 pairs of magnets, a spacer, and a printed circuit board including 2 coils.

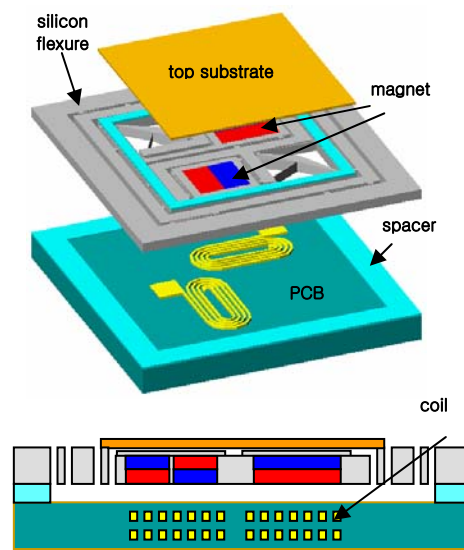


Figure 1: A schematic view of the stage

The flexure consists of many springs, 2 magnet holders for each of X and Y direction, an inner frame, a middle frame, and an outer frame as a mechanical ground. The middle frame is designed to translate only along y axis, while the inner frame can translate only along x axis relative to the middle frame. The rotator swings on its pivot when the magnet holder moves. So the inner and middle frames are forced to move in the opposite direction of the magnet holders as shown in Figure 2. The top substrate is attached to the inner frame and its motion can be controlled by applying a current in the coil. The mass and the dimension of the components including magnets are chosen to have no net torque around its pivot under an external acceleration, which results in a good vibration resistance.

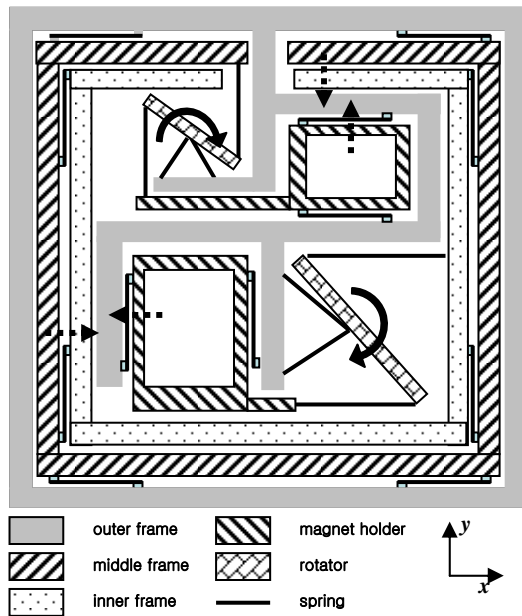


Figure 2: Anti vibration mechanism in the flexure

The frames are connected to each other by silicon beam springs with a high aspect ratio which allow a motion mainly in one direction. The separation of orthogonal motion and the high aspect ratio springs make it possible to realize a high robustness against external vibration along z-axis. A high fill factor of 45% is achieved by placing an anti vibration structure under the top substrate.

The top substrate which can be used for recording medium substrate is a size of 12.8 x 12.8 mm<sup>2</sup> in lateral dimension and is bonded on the inner frame.

Two pairs of NdFeB magnets are bonded in each hole by epoxy. The magnetization of all the magnets is along z axis but the magnetization direction of each magnet of a pair is opposite. The size of the magnet is determined to be 1.5 mm x 3 mm x 0.5 mm considering the interference between the magnet pairs and the net torque. The remanent magnetic field (Br) of the magnet is about 1.3 Tesla.

The motion of this device can be analyzed by a simple spring-mass-damping model in low frequency regime. The effective mass of the moving parts including the top substrate, the inner frame, 2 pairs of magnets, was designed to be about 40 mg and the target resonant frequency is 200 Hz. So the effective spring constant should be more than 250 N/m and the maximum force about 10 mN is required for a 40 μm displacement, the half target stroke of our device.

Finite element method (FEM) analysis was performed to decide a width of the silicon beam springs by a commercial FEM package, ANSYS version 5.3. A simple solid model including the silicon flexure, the magnets, the top substrate has been developed and the modal analysis reveals that the width of the silicon beam springs should be larger than 24 μm for more than 200 Hz of the first resonant frequency. In that case, the second resonance is found slightly higher than the first one and the motion is a translation along the x-axis. The higher modes such as in-plane rotation and out-of-plane motion are found above 3 kHz. The displacement from the external acceleration of 1 G (= 9.8 m/s<sup>2</sup>) is about 50 nm for x- and y-axis and 25 nm for z-axis. The crosstalk between the translations along x-axis and y-axis is below 10 nm.

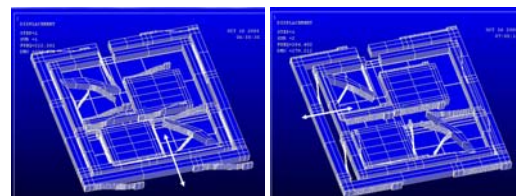


Figure 3: Modal analysis results (a) 1st mode 212 Hz (b) 2nd mode 264 Hz

The PCB includes two multilayered planar coils consisting of 4 layers of copper film, which generate Lorentz force to drive the magnet pair in each direction when currents are applied in the coils. The spacer with 100 μm thickness is inserted between the silicon frame and the PCB to keep an enough gap.

The electromagnetic force depends on magnetic field, applied current, and the length of coil. So the shape of the coil is optimized to reduce the power consumption, while generating required 10 mN from the above analysis. We assumed 10 layered PCB for a planar coil and the optimization was done according to the design rule of PCB. The minimum pitch of 0.2 mm was selected to reduce the current as low as possible, while the power consumption rarely depends on the pitch.

If the magnetic field doesn't decrease drastically by the distance from the magnets, more metal layers for the coil result in less power consumption. But the field calculation shows that the magnetic field decreases rapidly as the distance from the magnets increases. So, it is also important to decide an optimal number of conducting layers to reduce

the power consumption since the net electromagnetic force can be calculated by summation of the force from each layer.

The design rule requires the top and bottom layers are 18  $\mu\text{m}$  thick, while the intermediate layers are 36  $\mu\text{m}$  thick. The prepreg with 60  $\mu\text{m}$  thickness is inserted between the conducting layers. Fig. 4 shows the current and the power required for the coil with N metal layers. The current required to generate the target force decreases as the number of metal layers increases but the power consumption shows the minimum. The power consumption of 21 mW and the current of 50 mA are required for the coil with seven metal layers at the target stroke.

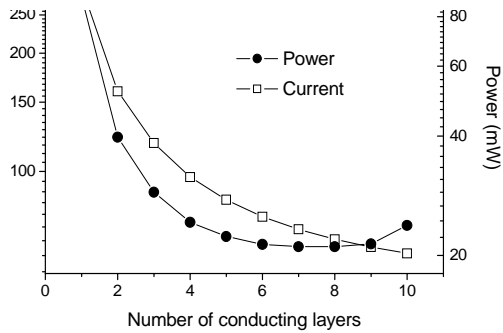


Figure 4: Optimization of the power consumption

### 3 FABRICATION

The process for the silicon frame begins with a four inch 350  $\mu\text{m}$  thick silicon wafer. The wet oxidation process is done to form 2  $\mu\text{m}$  thick silicon oxide film. The silicon oxide film is etched by inductive coupled plasma after photolithography as a mask for the following process. The exposed silicon is deep reactive ion etched (DRIE) thoroughly in Fig. 5 (a) in a low frequency mode to prevent footing effect. Then the wafer is diced into pieces and the magnet pairs are bonded in each holder as shown in Fig. 5 (b). Top substrate is bonded on the inner frame with epoxy. Finally the PCB with alumina spacer is bonded to the flexure as shown in Fig. 5 (d)

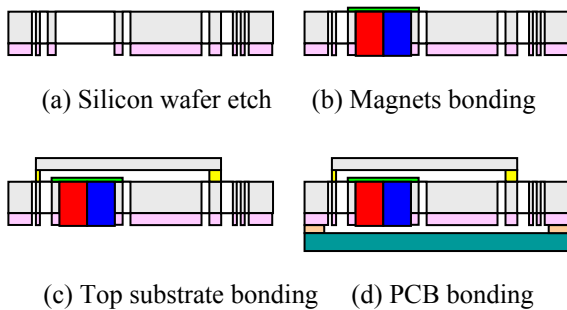


Figure 5: A schematic view of the fabrication process

There are only four metal layers instead of six layers in the PCB, though the coil with six layers consumes less power (See Fig. 6). It is because there is little improvement in power consumption while the total thickness of the device increases by more than 0.3 mm. It cannot be just ignored since the thickness of memory cards are very thin.

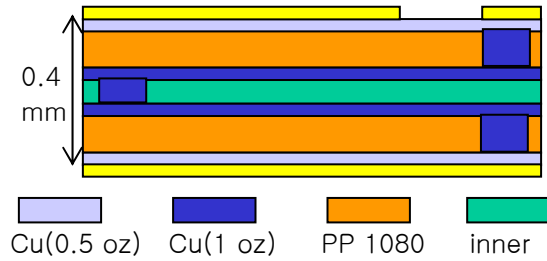
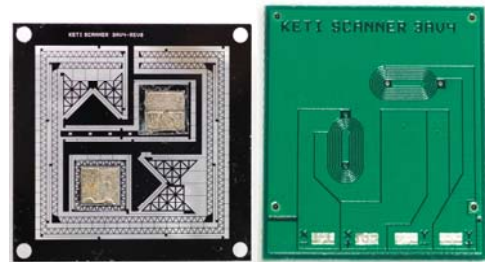
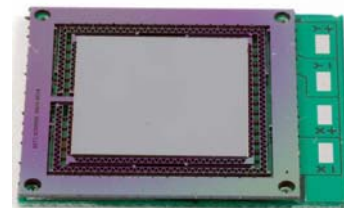


Figure 6: Layer structure of PCB

Fig. 7 (a) is a photograph of the silicon flexure after magnet bonding. The width of the springs varies from 20  $\mu\text{m}$  to 24  $\mu\text{m}$  while the designed width is 23  $\mu\text{m}$ , which happens during the silicon DRIE process. It is bonded on the PCB in Fig. 7(c). Fig. 7 (c) shows the stage after assembly. The total size of the device is 19.6 mm x 19.6 mm x 0.8 mm, which is compatible to SD memory card in size.



(a) silicon flexure with magnets (b) PCB



(c)

Figure 7: Components and stage fabricated

## 4 RESULTS

The PCB is connected with a high linearity current driver and function generator. The stage has been evaluated by optical microscope combined with a CCD for measuring the static displacement and dynamic response.

Fig. 8 is a graph showing a static response of the device. Good linearity has been achieved as shown in the graph. Since the full stroke of  $80\ \mu\text{m}$  is very small compared with the size of the magnets, we can assume the magnetic field around the coils remains nearly constant resulting in a linearity. The current of  $200\ \text{mA}$  is applied for the  $34\ \mu\text{m}$  stroke in the measurement. It is a little higher than the calculated value and it might be because the remanent field of the magnets decrease during the assembly process such as thermal curing of epoxy.

The measured resistance of the coil for one axis is about  $1.1\ \Omega$  and it matches well with the design. So, the peak power at  $34\ \mu\text{m}$  stroke is calculated to be  $44\ \text{mW}$  for one axis while the average power consumption for a  $\pm 34\ \mu\text{m} \times \pm 34\ \mu\text{m}$  linear scan is about  $29\ \text{mW}$ .

Fig. 9 shows a frequency response of the device. The first resonance frequency is  $186\ \text{Hz}$  which is smaller than the designed value. It is a result of the reduced width of the springs as mentioned in the fabrication section. The graph shows a high Q-factor about 20 but it should be reduced for a better servo control. No high order resonance below  $3\ \text{kHz}$  was observed and shows a dynamic response similar to a simple damped harmonic oscillator.

No crosstalk between the axes during the actuation was observed by optical microscope, but a precise measurement with a laser vibrometer will be required for quantitative analysis.

In addition, a good linearity of the actuator results in nano scale resolution of the stage, which was seen in qualitative imaging test with AFM system.

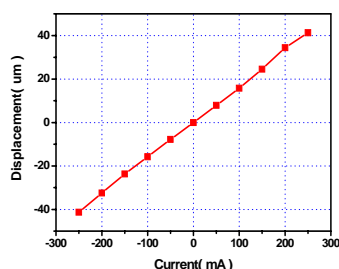


Figure 8: Optically measured lateral displacement for the as a function of the applied current in the coil.

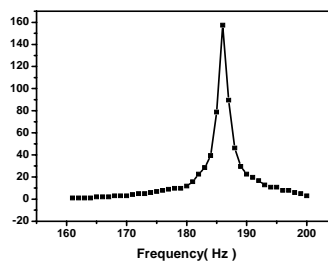


Figure 9: Frequency response of y axis by optical image analysis. The first resonance frequency is  $186\ \text{Hz}$ .

## 5 CONCLUSION

An electromagnetic XY stage has been fabricated and tested. The stage consists of a silicon frame, 2 pairs of magnets, a spacer, and a printed circuit board (PCB). The silicon frame was fabricated with conventional micromachining process and the design of PCB was optimized to reduce power consumption during operation. The total size of the device after integration is  $19.6 \times 23.2 \times 0.8\ \text{mm}^3$  while the stage area is  $12.8 \times 12.8\ \text{mm}^2$ . The measured displacement is  $\pm 34\ \mu\text{m}$  for input current of  $\pm 200\ \text{mA}$  (average power consumption is  $29\ \text{mW}$ ) and the resonance frequency is  $186\ \text{Hz}$ .

## REFERENCES

- [1] E. Eleftheriou, T. Antonakopoulos, G. K. Binnig, G. Cherubini, M. Despont, A. Dholakia, U. Dürig, M. A. Lantz, H. Pozidis, H. E. Rothuizen, and P. Vettiger, *IEEE Trans. Magnetics.*, 39 (2003) 938.
- [2] S. Gidon, O. Lemonnier, B. Rolland, O. Bichet, and C. Dressler, *Appl. Phys. Lett.* 85 (2004) 6392.
- [3] Y. Cho, K. Fujimoto, Y. Hiranaga, Y. Wagatsuma, A. Onoe, K. Terabe, and K. Kitamura, *Appl. Phys. Lett.*, 81 (2002) 4401.
- [4] C. H. Kim, H. M. Jeong, J. U. Jeon, and Y. K. Kim, *J. Microelectromech. Sys.* 53 (2003) 470.
- [5] Storrs Hoen, Qing Bai, Jonah A. Harley, David A. Horsley, Farid Matta, Tracy Verhoeven, Judy Williams, and Kirt R. Williams, *12th Int. Conf. Solid State Sens. Actua. Microsys.* (2003) 344.
- [6] H. G. Xu, K. Okamoto, D. Y. Zhang, T. Ono, and M. Esashi, *13th Int. Conf. Solid State Sens. Actua. Microsys.* (2005) 717.
- [7] J. J. Choi, H. Park, K. Y. Kim, J. U. Jeon, *J. Semicond. Tech. Sci.* 1 (2001) 84.
- [8] H. Rothuizen, U. Drechsler, G. Genolet, W. Haberle, M. Lutwyche, R. Stutz, R. Widmer, P. Vettiger, *Microelectron. Eng.* 53 (2000) 509.
- [9] A Pantazi, MA Lantz, G Cherubini, H Pozidis, and E Eleftheriou, *Nanotechnology* 15 (2004) S612.